SINGULARITY ANALYSIS OF A FAMILY OF KINEMATICALLY REDUNDANT PLANAR PARALLEL MANIPULATORS

Iman Ebrahimi[1], Juan A. Carretero[2], Roger Boudreau[3]

[1] *Dept. of Mechanical Engineering, University of New Brunswick, Iman.Ebrahimi@unb.ca*

[2] *Dept. of Mechanical Engineering, University of New Brunswick, Juan.Carretero@unb.ca*

[3] *Département de génie mécanique, Université de Moncton, Roger.A.Boudreau@umoncton.ca*

Abstract

Parallel manipulators feature relatively high payload and accuracy capabilities compared to their serial counterparts. However, they suffer from small workspace and low maneuverability. Kinematic redundancy for parallel manipulators can improve both of these characteristics. This paper presents a family of new kinematically redundant planar parallel manipulators with 6 degrees of freedom based on a 3-PRRR architecture obtained by adding an active prismatic joint at the base of each limb of the 3-RRR manipulator. First, the inverse displacement of the manipulators is explained and equations are derived. Then the Jacobian matrices of the manipulators are derived and different types of singularities are analysed and demonstrated. It is shown that the vast majority of singularities can be avoided by using kinematic redundancy.

Keywords: kinematic redundancy, planar parallel manipulators, inverse displacement, singularity analysis

ANALYSE DES SINGULARITÉS D'UN NOUVEAU MANIPULATEUR PARALLÈLE REDONDANT

Résumé

Les manipulateurs parallèles peuvent manipuler des charges plus élevées et ont une meilleure précision que les manipulateurs sériels. Cependant, leur espace de travail est plus restreint et ils ont moins de manoeuvrabilité. La redondance cinématique des manipulateurs parallèles peut améliorer ces deux caractéristiques. Cet article présente une famille de nouveaux manipulateurs parallèles plans redondants ayant six degrés de liberté basée sur une architecture 3-PRRR qui est obtenue par l'ajout d'un actionneur prismatique à la base de chaque chaîne d'un manipulateur de type 3-RRR. La solution du problème géométrique inverse des manipulateurs redondants est expliquée et résolue pour les manipulateurs présentés. Les matrices Jacobiennes des manipulateurs sont dérivées et les différents types de singularités sont analysés et démontrés. Il est montré que la majorité des singularités peuvent être évitées en utilisant la redondance cinématique.

Mots clés: redondance cinématique, manipulateurs parallèles plans, problème géométrique inverse, analyse de singularités

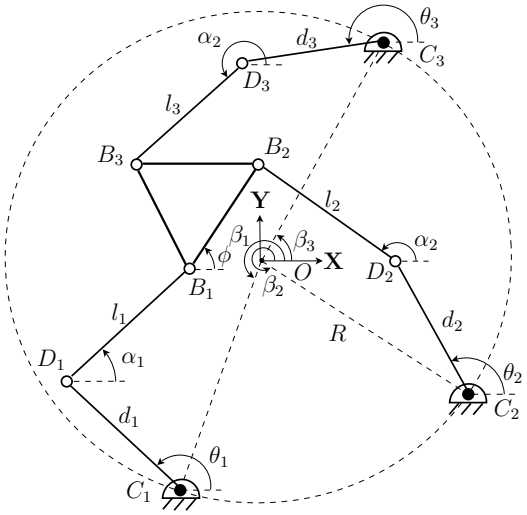

Figure 1: 3-RRR planar parallel manipulator.

1 INTRODUCTION

Higher accuracy, speed, and payload-to-weight ratio are the major advantages of parallel manipulators compared to serial manipulators. A smaller workspace, reduced dexterity, as well as complex kinematic and dynamic models, are their major drawbacks. Much research has been conducted on kinematics and dynamics of parallel manipulators [1]-[5], as well as on singularity analyses [6].

The vast majority of the studies on parallel manipulators have focused on non-redundant parallel manipulators. Redundant parallel manipulators have been introduced to alleviate some of the aforementioned shortcomings of parallel manipulators. Redundancy in parallel manipulators was first introduced in [7] and [8]. Redundancy can be divided into two main types: actuation redundancy and kinematic redundancy. *Actuation redundancy* is defined as replacing existing passive joints of a manipulator by active ones. Actuation redundancy does not change the mobility or reachable workspace of a manipulator but entails the manipulator having more actuators than are needed for a given task and may be used to reduce the singularities within the manipulator's workspace [9]. For example, the planar 3-RRR[4] parallel manipulator, shown in Figure 1, becomes redundantly actuated when a normally passive revolute joint such as B_i or D_i is replaced with an active joint. *Kinematic redundancy* increases the mobility and degrees of freedom (DOF) of parallel manipulators. Kinematic redundancy takes place when extra active joints and links (if needed) are added to manipulators. For instance, by adding one extra active prismatic joint to one limb of the 3-RRR, it is converted into a kinematically redundant parallel manipulator (see Figure 2). In this example, the resulting redundant parallel manipulator has 4-DOF, one more than the planar task space. In general, kinematic redundant parallel manipulators need more controlling parame-

[4]The terminology used is the following. A 3-RRR mechanism indicates that the end-effector is connected to the base by three serial kinematic chains (limbs), each consisting of an active (and therefore underlined) revolute joint (R) connected to the base, followed by two passive revolute joints, the second of which connects the limb to the end-effector. In the adopted notation, a prismatic joint would be shown by a P and would be underlined if it were active.

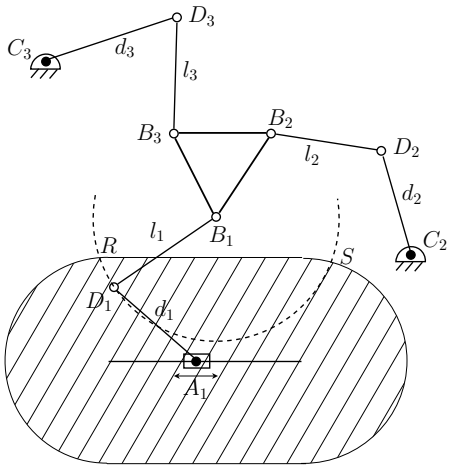

Figure 2: 4-DOF kinematically redundant planar parallel manipulator and its locus of solutions for the inverse displacement problem, shown as arc $\widehat{RD_1S}$.

ters than required for a set of given tasks [9]. A manipulator with sufficient kinematic redundancy can avoid all interior singularities, has a larger workspace and improved maneuverability [10]. Using kinematic redundancy can also allow manipulators to cope with joint-jam failure (*e.g.*, [11]).

Compared to other research that has been pursued for parallel manipulators, redundancy in such manipulators has not adequately been studied. In serial manipulators, the concept of kinematic redundancy has been broadly studied (see for instance [12]).

In the present work, a family of 6-DOF kinematically redundant planar parallel manipulators is introduced. First, the proposed 3-PRRR manipulator family obtained by adding an active prismatic joint at the base of each limb of a 3-RRR manipulator is presented. Then, their inverse displacement problem (IDP) is explained. Finally, the direct, inverse and combined singularities of the aforementioned manipulators are analysed and illustrated.

2 PROPOSED ARCHITECTURES

Adding one degree of kinematic redundancy (1-DOKR) can considerably reduce the number of direct singularities of a 3-RRR planar manipulator but not all of them [9]. By adding 2-DOKR, it is possible to avoid all direct singularities of the 3-RRR manipulators. A symmetrical architecture is usually desirable. Also as is shown later, kinematic redundancy increases the workspace, hence, 1-DOKR is added here to each limb of the 3-RRR manipulator producing manipulators with a total of 3-DOKR. Therefore, the family of redundant manipulators proposed here has 6-DOF for a planar task, three of which are redundant. The added kinematic redundancies enable the manipulators to avoid singularities, improve their maneuverability, and enlarge their reachable and dexterous workspaces.

Figures 3 to 5 illustrate a new family of three 6-DOF redundant planar parallel manipulators. The notation used for each manipulator is based on the shape of the guides on which the redundant prismatic actuators slide. All 3-PRRR manipulators are based on the non-redundant 3-RRR planar parallel manipulator proposed in [14] (Figure 1). Each limb of the 3-PRRR manipulators has one

prismatic actuator at its base. Adding prismatic redundant actuators close to the base causes less dynamic effects due to the weight of the actuators.

The redundant prismatic actuators slide on their respective guides that can take the shape of a triangle, a star, and a circle. The notation is thus 3-PRRR$_{\triangle}$, 3-PRRR$_{\bigstar}$ and 3-PRRR$_{\bigcirc}$ for guides that have a triangle, star or circle shape, respectively. An actuated revolute joint is mounted on the prismatic actuator at point A_i (throughout the present work, $i = 1, 2, 3$). Note that the solid circles in all the figures represent active revolute joints whereas the empty circles represent passive ones. Finally, two passive revolute joints are at D_i and B_i, where point B_i is attached to the end-effector.

3 INVERSE DISPLACEMENT OF THE PROPOSED ARCHITECTURES

Kinematic redundancy in manipulators results in having an infinite number of solutions to the inverse displacement problem. That is, rather than having a finite number of solutions, there may be one or more loci of joint variable values (angles or lengths) for a given position and orientation of the end-effector. Figure 2 illustrates a situation where, by adding an extra prismatic actuator to the first limb, 1-DOKR is added to that limb of a 3-RRR planar parallel manipulator. The resulting kinematically redundant manipulator has 4-DOF for a planar task. That is, as long as two circles centred at B_1 and A_1 and radii of l_1 and d_1, respectively, intersect each other, there are infinite solutions for the inverse displacement problem of the manipulator.

The hatched region in Figure 2 shows the area that point D_1 of link A_1D_1 can cover when the prismatic actuator A_1 slides within a certain range and link A_1D_1 rotates around point A_1. As it is evident from Figure 2, point D_1 as a part of link B_1D_1 (pinned at point B_1) can rotate a full circle around point B_1. Therefore, all possible solutions of the inverse displacement problem for that limb lie on the intersection of the aforesaid regions. Assuming that the IDP exists for limb 1, the redundant manipulator has a locus of solutions shown as arc $\widehat{RD_1S}$. Note that the inverse displacement problem for each limb of the original non-redundant 3-RRR has at the most two solutions.

Finding the best inverse displacement solution for redundant manipulators is normally formulated as a numerical optimisation problem [12]. To find an optimal solution of the IDP, different cost functions may be defined for different purposes such as minimum energy, distance, time or condition number [12] and [13]. Note that once a position for one of the active joints A_i or θ_i is chosen, there are only two solutions for the IDP of each limb for a given position and orientation of the end-effector.

Figure 6 shows the details of the end-effector and its associated dimensions which are the same for all the manipulators. Considering the end-effector location is measured from point P and the geometry of the 3-PRRR manipulator family as shown in Figures 3 to 6, the IDP of the manipulator can be written as

$$\overline{D_iB_i} = \overline{D_iA_i} + \overline{A_iO} + \overline{OP} + \overline{PB_i} \tag{1}$$

Equation (1) can be expressed as

$$x_{\overline{D_iB_i}}{}^2 + y_{\overline{D_iB_i}}{}^2 = x_{(\overline{D_iA_i}+\overline{A_iO}+\overline{OP}+\overline{PB_i})}{}^2 + y_{(\overline{D_iA_i}+\overline{A_iO}+\overline{OP}+\overline{PB_i})}{}^2 \tag{2}$$

$$x_{\overline{D_iB_i}}{}^2 + y_{\overline{D_iB_i}}{}^2 = {l_i}^2 \tag{3}$$

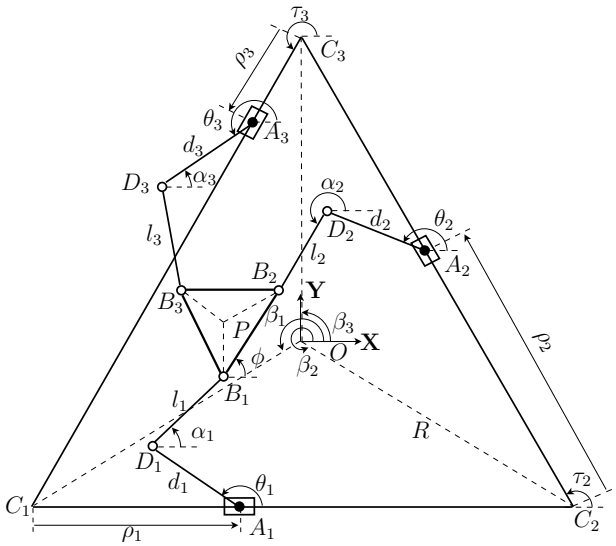

Figure 3: 3-PRRR$_{\Delta}$ planar 6-DOF kinematically redundant parallel manipulator.

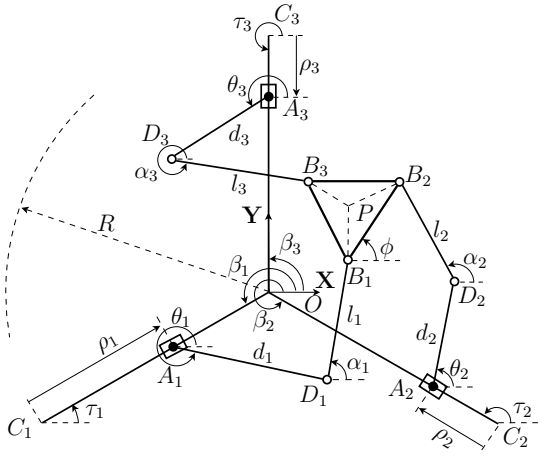

Figure 4: 3-PRRR$_{\bigstar}$ planar 6-DOF kinematically redundant parallel manipulator.

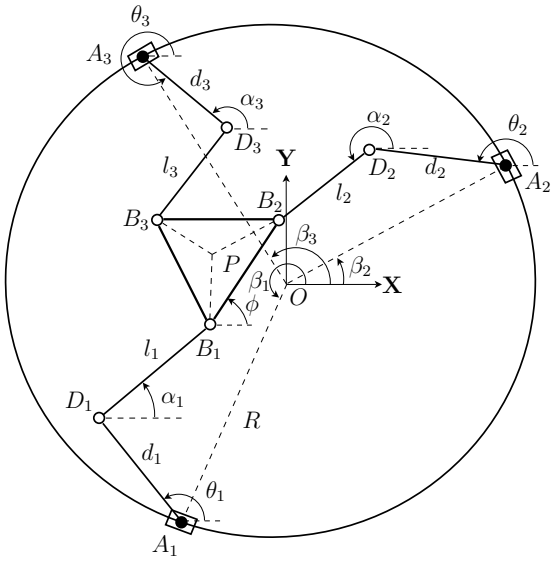

Figure 5: 3-PRRR$_{\bigcirc}$ planar 6-DOF kinematically redundant parallel manipulator.

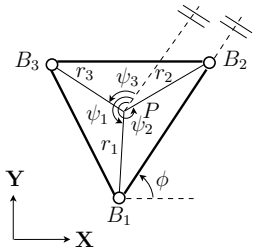

Figure 6: End-effector details for all the manipulators.

For the 3-PRRR$_\triangle$ and the 3-PRRR$_\bigstar$ manipulators, the inverse displacement equations can be written as

$$\begin{aligned} l_i^2 = &(x_p + r_i c_{(\phi+\psi_i)} - R c_{\beta_i} - \rho_i c_{\tau_{i_{\triangle,\bigstar}}} - d_i c_{\theta_i})^2 \\ &+(y_p + r_i s_{(\phi+\psi_i)} - R s_{\beta_i} - \rho_i s_{\tau_{i_{\triangle,\bigstar}}} - d_i s_{\theta_i})^2 \end{aligned} \tag{4}$$

where $c_\measuredangle$ and $s_\measuredangle$ represent $\cos(\measuredangle)$ and $\sin(\measuredangle)$, respectively. All angles except ψ_i (which is measured relative to B_1B_2, see Figure 6) are measured with respect to the *X*-axis. Also, a double architecture identification symbol indicates the angle to be used depending on the considered kinematic architecture. For example $c_{\tau_{3_{\triangle,\bigstar}}}$ refers to the cosine of $\tau_{3_\triangle}$ or $\tau_{3_\bigstar}$ depending on the architecture. Angles τ_i are defined as

$$\begin{aligned} \tau_{1_\triangle} &= 0 & \qquad \tau_{1_\bigstar} &= \tfrac{\beta_1-\beta_2+\pi}{2} \\ \tau_{2_\triangle} &= \tfrac{\beta_3-\beta_1+2\pi}{2} & \qquad \tau_{2_\bigstar} &= \tfrac{\beta_2-\beta_1+\pi}{2} \\ \tau_{3_\triangle} &= \tfrac{\beta_3-\beta_2+4\pi}{2} & \qquad \tau_{3_\bigstar} &= \tfrac{2\beta_3-\beta_2-\beta_1+\pi}{2} \end{aligned}$$

Similarly, for the 3-PRRR$_\bigcirc$ manipulator, the inverse displacement equations can be written as

$$l_i^2 = (x_p + r_i c_{(\phi+\psi_i)} - R c_{\beta_i} - d_i c_{\theta_i})^2 + (y_p + r_i s_{(\phi+\psi_i)} - R s_{\beta_i} - d_i s_{\theta_i})^2 \tag{5}$$

For the 3-PRRR$_\triangle$ and 3-PRRR$_\bigstar$ manipulators, the end-effector pose and the actuator vectors can be expressed as $\mathbf{x} = [x_p, y_p, \phi]^T$ and $\mathbf{q} = [\rho_1, \theta_1, \rho_2, \theta_2, \rho_3, \theta_3]^T$, respectively. For the 3-PRRR$_\bigcirc$ manipulator, they can be defined as $\mathbf{x} = [x_p, y_p, \phi]^T$ and $\mathbf{q} = [\beta_1, \theta_1, \beta_2, \theta_2, \beta_3, \theta_3]^T$, respectively.

Regardless of the optimisation method that is chosen, the selected inverse displacement solution depends on the initial pose and configuration of each limb as well as the cost function that is used [10; 13]. This work mainly focuses on introducing a family of kinematically redundant planar manipulators and analysing the manipulators' singularities. Optimal path selection is an extensive topic on its own and is left for subsequent research.

4 SINGULARITY ANALYSIS

Jacobian matrices transform the velocity vector of the end-effector into a velocity vector of the active joints. That is,

$$\mathbf{J_x}\dot{\mathbf{x}} = \mathbf{J_q}\dot{\mathbf{q}} \tag{6}$$

where $\dot{\mathbf{x}}$ is the velocity vector of the end-effector and $\dot{\mathbf{q}}$ is the velocity vector of the associated active joints. Considering equation (6), three types of singularities can be defined for parallel manipulators [16]:

1. Direct kinematic singularities when $\mathbf{J_x}$ is singular.
2. Inverse kinematic singularities when $\mathbf{J_q}$ is singular.
3. Combined (complex) singularities when $\mathbf{J_x}$ and $\mathbf{J_q}$ are singular.

Direct singularities (*i.e.*, $|\mathbf{J_x}| = 0$) take place when there are some nonzero velocities of the end-effector that are possible with zero velocities at the actuators. Also, direct kinematic singularities are referred to as force uncertainties or as force unconstrained poses [17]. On the other hand, inverse singularities (*i.e.*, when $|\mathbf{J_q}| = 0$) happen when there exist some nonzero actuator velocities that cause zero velocities for the end-effector. In order to perform a singularity analysis on the introduced 3-PRRR manipulator family, their Jacobian matrices are obtained in the following section.

4.1 Jacobian matrices of the 3-PRRR manipulators

By differentiating equation (4) with respect to time, the Jacobian matrices are given by:

$$\mathbf{J}_{\mathbf{x}_\forall} = \begin{bmatrix} t_{11_\forall} & t_{12_\forall} & t_{13_\forall} \\ t_{21_\forall} & t_{22_\forall} & t_{23_\forall} \\ t_{31_\forall} & t_{31_\forall} & t_{33_\forall} \end{bmatrix}_{3\times 3} \tag{7}$$

$$\mathbf{J}_{\mathbf{q}_\forall} = \begin{bmatrix} u_{1_\forall} & v_{1_\forall} & 0 & 0 & 0 & 0 \\ 0 & 0 & u_{2_\forall} & v_{2_\forall} & 0 & 0 \\ 0 & 0 & 0 & 0 & u_{3_\forall} & v_{3_\forall} \end{bmatrix}_{3\times 6} \tag{8}$$

where $\forall = \Delta, \bigstar, \bigcirc$, depending on the manipulator. For the 3-PRRR$_\Delta$ and 3-PRRR$_\bigstar$ manipulators the elements are

$t_{i1_{\Delta,\bigstar}} = x_p + r_i c_{(\phi+\psi_i)} - R c_{\beta_i} - \rho_i c_{\tau_{i_{\Delta,\bigstar}}} - d_i c_{\theta_i}$
$t_{i2_{\Delta,\bigstar}} = y_p + r_i s_{(\phi+\psi_i)} - R s_{\beta_i} - \rho_2 s_{\tau_{2_{\Delta,\bigstar}}} - d_i s_{\theta_i}$
$t_{i3_{\Delta,\bigstar}} = -r_i s_{(\phi+\psi_i)} t_{i1_{\Delta,\bigstar}} + r_i c_{(\phi+\psi_i)} t_{i2_{\Delta,\bigstar}}$

$u_{i_{\Delta,\bigstar}} = c_{\tau_{i_{\Delta,\bigstar}}} t_{i1_{\Delta,\bigstar}} + s_{\tau_{i_{\Delta,\bigstar}}} t_{i2_{\Delta,\bigstar}}$
$v_{i_{\Delta,\bigstar}} = -d_i s_{\theta_i} t_{i1_{\Delta,\bigstar}} + d_i c_{\theta_1} t_{i2_{\Delta,\bigstar}}$

whereas for the 3-PRRR$_\bigcirc$ the elements are

$t_{i1_\bigcirc} = x_p + r_i c_{(\phi+\psi_i)} - R c_{\beta_i} - d_i c_{\theta_i}$
$t_{i2_\bigcirc} = y_p + r_i s_{(\phi+\psi_i)} - R s_{\beta_i} - d_i s_{\theta_i}$
$t_{i3_\bigcirc} = -r_i s_{(\phi+\psi_i)} t_{i1_\bigcirc} + r_i c_{(\phi+\psi_i)} t_{i2_\bigcirc}$

$u_{i_\bigcirc} = -R s_{\beta_i} t_{i1_\bigcirc} + R c_{\beta_i} t_{i2_\bigcirc}$
$v_{i_\bigcirc} = -d_i s_{\theta_i} t_{i1_\bigcirc} + d_i c_{\theta_i} t_{i2_\bigcirc}$

4.2 Direct kinematic singularities of the 3-PRRR manipulators

The direct kinematic singularities of planar parallel manipulators with architectures whose distal links have passive revolute joints at both ends are the same. They all take place when the lines defining the distal links meet at a common point. The reason for this is that forces can only be transmitted in the distal link directions, and, when all of them meet at a common point, the end-effector can rotate around that point infinitesimally while all the actuators are locked. As shown in

Figures 3 to 5, all manipulators have passive revolute joints at both ends of the distal links (*i.e.*, B_i and D_i).

The direct Jacobian matrix of all manipulators can be re-written as:

$$\mathbf{J}_{\mathbf{x}_\forall} = \begin{bmatrix} x_{l_1} & y_{l_1} & -r_1 s_{(\phi+\psi_1)} x_{l_1} + r_1 c_{(\phi+\psi_1)} y_{l_1} \\ x_{l_2} & y_{l_2} & -r_2 s_{(\phi+\psi_2)} x_{l_2} + r_2 c_{(\phi+\psi_2)} y_{l_2} \\ x_{l_3} & y_{l_3} & -r_3 s_{(\phi+\psi_3)} x_{l_3} + r_3 c_{(\phi+\psi_3)} y_{l_3} \end{bmatrix}_{3\times 3} = \begin{bmatrix} l_1 c_{\alpha_1} & l_1 s_{\alpha_1} & r_1 l_1 s_{(\alpha_1-\phi-\psi_1)} \\ l_2 c_{\alpha_2} & l_2 s_{\alpha_2} & r_2 l_2 s_{(\alpha_2-\phi-\psi_2)} \\ l_3 c_{\alpha_3} & l_3 s_{\alpha_3} & r_3 l_3 s_{(\alpha_3-\phi-\psi_3)} \end{bmatrix}_{3\times 3} \tag{9}$$

where x_{l_i} and y_{l_i} are the projections of links $B_i D_i$ onto the X and Y axes, respectively. The determinant of $\mathbf{J}_{\mathbf{x}_\forall}$ is zero, when there are linear dependencies between any two or more rows or columns. That is,

$$\lambda_1 \mathbf{\Gamma}_1 + \lambda_2 \mathbf{\Gamma}_2 + \lambda_3 \mathbf{\Gamma}_3 = 0 \tag{10}$$

where λ_i are scalar coefficients of linear dependency of which only up to two can be zero simultaneously and vector $\mathbf{\Gamma}_i$ represents the ith row (or column) of $\mathbf{J}_{\mathbf{x}_\forall}$. Having only one λ_i nonzero represents configurations where all the elements of a row or a column are zero. Considering equation (9), the elements of the first or second column are zero when $x_{l_i} = 0$ or $y_{l_i} = 0$, respectively. These two conditions occur when all the distal links are parallel to the *Y*-axis or *X*-axis, respectively. In both cases, the distal links meet at a common point at infinity. The third column becomes zero, when all the distal links meet at point P. Also, linear dependency between the rows have the same meaning as columns. Linear dependency between any two rows happens when two distal links are aligned with the side of the end-effector that is between them. Note that singularities are independent of the coordinate system. For the discussed manipulators, a singularity configuration only depends on relative positions and orientations of the distal links. Therefore, the aforementioned direct singularities can take place when all the distal links are parallel regardless of the common direction or where they all meet at a common point.

4.3 Inverse kinematic singularities of the 3-PRRR manipulators

For redundant parallel manipulators, the matrix $\mathbf{J}_{\mathbf{q}_\forall}$ is not square, and therefore, the inverse kinematic singularities can be said to occur when the rank of $\mathbf{J}_{\mathbf{q}_\forall}$ is lower than the DOF of the end-effector [8], that is, the number of rows of $\mathbf{J}_{\mathbf{q}_\forall}$. Therefore, a kinematically redundant parallel manipulator is in an inverse singular configuration when any minor square matrix extracted from $\mathbf{J}_{\mathbf{q}_\forall}$ is singular. This degeneracy can also be identified as the condition that sets the determinant of $\mathbf{J}_{\mathbf{q}_\forall}\mathbf{J}_{\mathbf{q}_\forall}{}^T$ to zero. For the family of manipulators being presented,

$$\mathbf{J}_{\mathbf{q}_\forall}\mathbf{J}_{\mathbf{q}_\forall}{}^T = \begin{bmatrix} u_1^2 + v_1^2 & 0 & 0 \\ 0 & u_2^2 + v_2^2 & 0 \\ 0 & 0 & u_3^2 + u_3^2 \end{bmatrix}_{3\times 3} \tag{11}$$

The elements of the matrix in equation (11) for the 3-PRRR$_\Delta$ and the 3-PRRR$_\bigstar$ can be expressed as

$$u_{i_{\Delta,\bigstar}} = l_i c_{(\alpha_i-\tau_i)} \qquad\qquad v_{i_{\Delta,\bigstar}} = d_i l_i s_{(\alpha_i-\theta_i)}$$

whereas those for the 3-PRRR$_\bigcirc$ can be expressed as

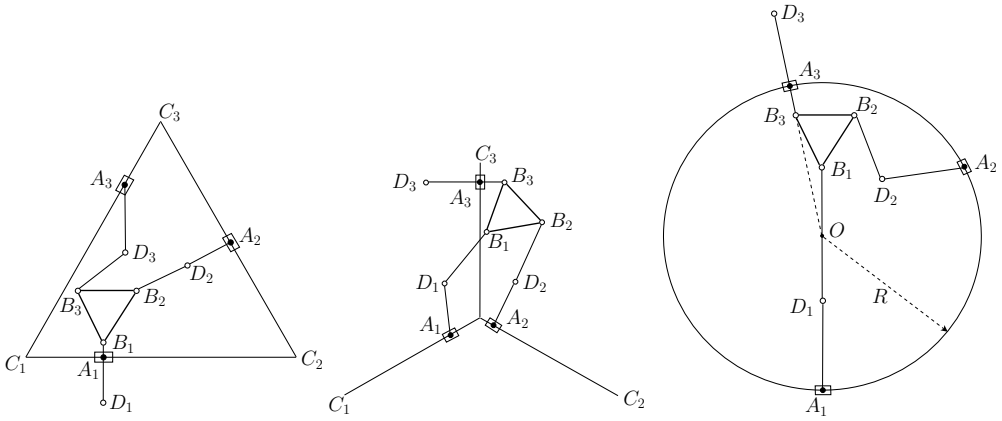

a) 3-PRRR$_\triangle$ b) 3-PRRR$_\bigstar$ c) 3-PRRR$_\bigcirc$

Figure 7: Examples of the geometrical interpretations of the inverse kinematic singularities for the 3-PRRR manipulators.

$$u_{i_\bigcirc} = Rl_i s_{(\alpha_i - \beta_i)} \qquad v_{i_\bigcirc} = d_i l_i s_{(\alpha_i - \theta_i)}$$

Since matrix $\mathbf{J}_{\mathbf{q}_\forall}\mathbf{J}_{\mathbf{q}_\forall}^T$ is diagonal, its determinant becomes zero when any one or more of the diagonal elements become zero. That is, $u_{i_\forall}^2$ and $v_{i_\forall}^2$ would have to be zero simultaneously. For the 3-PRRR$_\triangle$ and the 3-PRRR$_\bigstar$ manipulators, each diagonal element would be zero when both of the following conditions are satisfied:

$$\begin{array}{cc} \alpha_{i_{\triangle,\bigstar}} = \frac{2n_1+1}{2}\pi + \tau_{i_{\triangle,\bigstar}} & \text{AND} \quad \alpha_{i_{\triangle,\bigstar}} = n_2\pi + \theta_{i_{\triangle,\bigstar}} \\ n_1 = 0, 1, 2, ... & \qquad\qquad n_2 = 0, 1, 2, ... \end{array}$$

The above conditions show that inverse kinematic singularities for the 3-PRRR$_\triangle$ and 3-PRRR$_\bigstar$ manipulators occur when the sliding paths of the prismatic actuators (*i.e.*, C_iC_{i+1} for the 3-PRRR$_\triangle$ and C_iO for the 3-PRRR$_\bigstar$ manipulators) are perpendicular to B_iD_i and also limb $A_iD_iB_i$ is fully stretched or fully folded (*i.e.*, $A_iD_i \| D_iB_i$), as shown in Figures 7a and 7b.

For the 3-PRRR$_\bigcirc$ manipulator, each diagonal element of $\mathbf{J}_{\mathbf{q}_\forall}\mathbf{J}_{\mathbf{q}_\forall}^T$ becomes zero when both of the following conditions are satisfied

$$\begin{array}{cc} \alpha_{i_\bigcirc} = n_1\pi + \beta_{i_\bigcirc} & \text{AND} \quad \alpha_{i_\bigcirc} = n_2\pi + \theta_{i_\bigcirc} \\ n_1 = 0, 1, 2, ... & \qquad\qquad n_2 = 0, 1, 2, ... \end{array}$$

The above conditions for the inverse kinematic singularities of the 3-PRRR$_\bigcirc$ imply that the inverse kinematic singularities take place when at least one limb is fully stretched or fully folded and also passes through the centre of the circle (*i.e.*, point O). Figure 7c illustrates an inverse singular configuration when the first and third limbs are fully stretched and fully folded, respectively, and also pass through the centre of the guide's circle for the prismatic actuators. It should be noted that for the entire family of 3-PRRR manipulators, as long as the manipulator is not in its workspace boundary, it is possible to choose one or more sets of joint displacements that avoid the inverse singularity conditions outlined here.

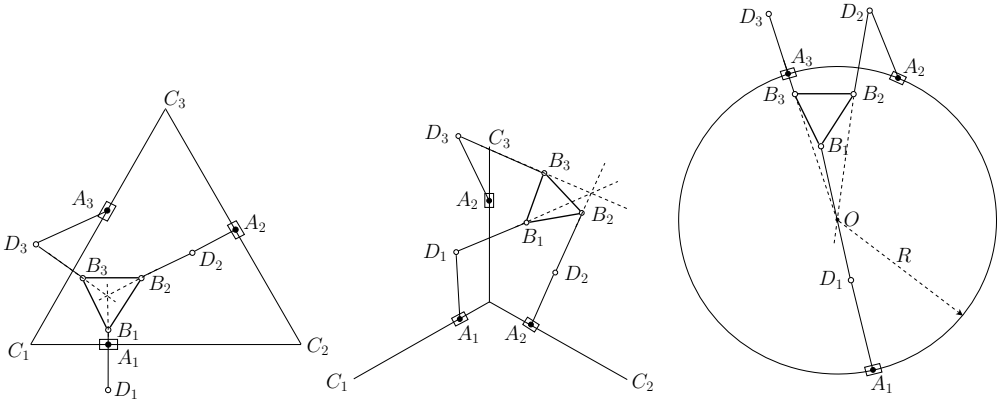

a) 3-PRRR$_{\triangle}$ b) 3-PRRR$_{\bigstar}$ c) 3-PRRR$_{\bigcirc}$

Figure 8: Examples of the geometrical interpretations of the combined kinematic singularities for the 3-PRRR manipulators.

4.4 Combined (complex) singularities of the 3-PRRR manipulators

The combined singularities happen when both direct and inverse kinematic singularities take place. In other words, when both $\mathbf{J}_{\mathbf{x}_\forall}$ and $\mathbf{J}_{\mathbf{q}_\forall}\mathbf{J}^T_{\mathbf{q}_\forall}$ are singular. Figures 8a, 8b and 8c show sample configurations in which both the direct and inverse singularities occur at the same time for the three manipulator of the 3-PRRR family introduced here.

5 CONCLUSIONS

A family of kinematically redundant planar parallel manipulators was proposed. Their inverse displacement problems were explained. Thereafter, the singularity analyses were presented and their geometrical interpretations were explained for the 3-PRRR manipulator family. It can be concluded that generally, inverse singularities occur for the whole family of 3-PRRR manipulators when at least one limb is fully stretched or fully folded while the limb is perpendicular to the sliding direction of the prismatic actuator, *i.e.*, when the entire limb is collinear with the line that passes through the centre of curvature of the slider's path at that point. Generally the proposed manipulators have loci of solutions for every pose inside their workspaces. Therefore, they have the capability to be programmed to optimise different cost functions such as minimum time, energy, while constrained to avoid singularities.

REFERENCES

[1] M. G. Mohamed and J. Duffy. Direct determination of the instantaneous kinematics of fully parallel robot manipulators. *Journal of Mechanisms, Transmissions and Automation in Design*, 107(2):226–229, 1985.

[2] T. Yoshikawa. Manipulability of robot mechanisms. *International Journal of Robotics Research*, 4(2):3–9, 1985.

[3] F. Tahmasebi and L.-W. Tsai. Closed-form direct kinematics solution of a new parallel min-

imanipulator. *Journal of Mechanical Design, Transactions of the ASME,* 116(4):1141–1147, 1994.

[4] K. Zanganeh and J. Angeles. Instantaneous kinematics of general hybrid parallel manipulators. *Journal of Mechanical Design,* 117(4):581–588, 1995.

[5] C. M. Gosselin. Parallel computational algorithms for the kinematics and dynamics of planar and spatial parallel manipulators. *Journal of Dynamic Systems, Measurement, and Control*, 118:22–28, March 1996.

[6] J. Sefrioui and C. M. Gosselin. Singularity analysis and representation of planar parallel manipulators. *Journal of Robotics and Autonomous Systems*, 10(4):209–224, 1992.

[7] S. Lee and S. Kim. Kinematic analysis of generalized parallel manipulator systems. *Proceedings of the IEEE Conference on Decision and Control*, 2:1097–1102, 1993.

[8] J.-P. Merlet. Redundant parallel manipulators. *Laboratory Robotics and Automation*, 8(1):17–24, 1996.

[9] J. Wang and C. M. Gosselin. Kinematic analysis and design of kinematically redundant parallel mechanisms. *Journal of Mechanical Design*, 126(1):109–118, 2004.

[10] I. Ebrahimi, and J. A. Carretero and R. Boudreau. 3-PRRR redundant planar parallel manipulator: inverse displacement, workspace and singularity analyses. *Mechanism and Machine Theory*, doi:10.1016/j.mechmachtheory.2006.07.006., available online.

[11] M. Hassan and L. Notash. Analysis of active joint failure in parallel robot manipulators. *Journal of Mechanical Design,* 126(6):959–968, 2004.

[12] Y. Nakamura. *Advanced robotics: redundancy and optimization*. Addison-Weslay Publishing Co., Reading, Massachusetts, USA, 1991.

[13] I. Ebrahimi, and J. A. Carretero, and R. Boudreau. Path Planning for the 3-PRRR Redundant Planar Parallel Manipulator. Accepted for Publication in *Proceedings of the 2007 IFToMM World Congress*, 2007.

[14] C. M. Gosselin and J. Angeles. The optimum kinematic design of a planar three-degree-of-freedom parallel manipulator. *ASME Journal of Mechanisms, Transmissions and Automation in Design*, 110(1):35–41, 1988.

[15] J.-P. Merlet, Parallel robots, Springer, 2nd Edition, 2006.

[16] C. M. Gosselin, J. Angeles, Singularity analysis of closed-loop kinematic chains. *IEEE Transactions on Robotics and Automation*, 6 (3) (1990) 281–290.

[17] F. Firmani, R. P. Podhorodeski, Force-unconstrained poses of the 3-PRR and 4-PRR planar parallel manipulators. *CSME Transactions*, 29 (4) (2005) 617–628